DOI: 10.1002/ejic.201100797

Ni-2,3-thiophenedithiolate Anions in New Architectures: An In-Line Mixed-Valence Ni Dithiolene (Ni_4–S_{12}) Cluster

Ana I. S. Neves,[a] Isabel C. Santos,[a] Laura C. J. Pereira,[a] Concepció Rovira,[b] Eliseo Ruiz,[c] Dulce Belo,*[a] and Manuel Almeida*[a]

Keywords: Nickel / Cluster compounds / Crown compounds / Magnetic properties / S ligands / Sulfur heterocycles

A family of salts that was based on the $[Ni(\alpha\text{-tpdt})_x]^{n-}$ anions (α-tpdt = 2,3-thiophenedithiolate) and the K^+ crown-ether cations were prepared and were then structurally and magnetically characterised. In $[K(18\text{-crown-6})][Ni(\alpha\text{-tpdt})_2]$, the anion has a square planar coordination geometry with ligand disorder and the cations and anions are segregated in alternating layers in the crystal structure, as was found in the previous $[Ni(\alpha\text{-tpdt})_2]^-$ salts. Two salts were obtained with the $[K(15\text{-crown-5})_2]^+$ cation. The expected 1:1 salt was obtained, which had the usual anion square planar coordination geometry for $[Ni(\alpha\text{-tpdt})_2]^-$ but that had a new molecular arrangement based on an anion double chain. In addition, a 2:1 salt was obtained, which had a new anionic geometry, namely, $[Ni_4(\alpha\text{-tpdt})_6]^{2-}$, which is an unprecedented example of an in-line mixed-valence Ni_4 dithiolene (Ni_4–S_{12}) cluster. A compound with an eight-membered tetrasulfide ring, namely a bis(thiophene-2,3-diyl) bis(sulfide), was also obtained. The salts that are based on the paramagnetic $[Ni(\alpha\text{-tpdt})_2]^-$ anion presented interesting magnetic properties that resulted from the competition between the antiferromagnetic (AFM) and ferromagnetic (FM) interactions with a low-temperature cluster glass behaviour, which was associated with the *cis-trans* ligand disorder.

Introduction

Transition metal dithiolene (dt) complexes, $M(dt)_n$, have attracted interest for more than 30 years due to their redox behaviour and rich structural diversity. They have been used successfully as the building blocks for molecular materials that have unconventional electrical and magnetic properties.[1] These dithiolene complexes are known to display a variety of coordination geometries that depend on the metal and specific preparative conditions. Most of the bidithiolene complexes of the metals from groups 8 to 11 adopt a square planar coordination geometry, $M(dt)_2$.[2] For some metals, however, such as Fe, Co, Pt and Ni, the tendency is to form a dimeric arrangement, $[M(dt)_2]_2$, by the formation of two M–S apical bonds in which the metal has a 4+1 coordination geometry.[1,3] In the case of the cobalt complexes trimeric $[M(dt)_2]_3$[4] and even polymeric $[M(dt)_2]_n$[5] arrangements are known where dt = mnt (mnt = maleonitriledithiolate). In these situations the metals can have different or partial formal oxidation states, which are stabilised by the significant contribution of the extended π-ligands to the frontier orbitals.

In terms of the Ni dithiolene complexes, a bimetallic $[M_2(dt)_3]_2$ cluster, which has a relatively short Ni–Ni bond (2.714–2.914 Å), has been reported for the ligands dmit (2-thione-1,3-dithiole-4,5-dithiolate)[6] and edt (ethane-1,2-dithiolate).[7] Other heteroleptic polynuclear Ni_3 and Ni_5 complexes, in which the dmit ligand is combined with the edt or pdt (propane-1,2-dithiolate) ligands, are also known but in these cases the Ni atoms are bridged by the S atoms and have no direct, short Ni–Ni bonds.[8] The four-centred tetrahedral clusters are only known to occur for copper, $[Cu_4(dt)_3]_2^{2-}$, and only with some of the dithiolate ligands and under specific conditions.[9]

In this paper we report on the synthesis of Ni complexes that have the thiophene-2,3-dithiolate ligand (α-tpdt) with a K^+ crown-ether counterion, which led to new molecular materials and structural architectures. The paramagnetic $[Ni(\alpha\text{-tpdt})_2]^-$ complex has already proved to be a suitable building block for molecular materials[10] but the role of the K^+ crown-ether cations, which acts as a linker between the paramagnetic units or induces new supramolecular structures, has not been explored previously in the crystal engineering of these materials. Among the new compounds and novel architectures that were obtained, which are described in this paper, there is a remarkable linear mixed-valence Ni_4 cluster, which is unprecedented among the metal-dithiolene complexes. In this case the Ni atoms present formal oxi-

[a] Department of Chemistry, Instituto Tecnológico e Nuclear/CFMC-UL,
Estrada Nacional no. 10, 2686-953 Sacavém, Portugal
Fax: +351-219946185
E-mail: malmeida@itn.pt
[b] Institut de Ciència des Materials de Barcelona (CSIC) and CIBER-BBN, Campus Universitari de Bellaterra,
08193 Cerdanyola, Spain
[c] Departament de Química Inorgànica and Institut de Recerca de Química, Teòrica i Computacional, Universitat de Barcelona, Diagonal 647, 08028 Barcelona, Spain

dation states of II and III and are at relatively short Ni–Ni distances.

Results and Discussion

A series of new compounds that are based on nickel complexes with the thiophene-2,3-dithiolate ligand and the crown-ethers cations, $[K(18\text{-crown-6})]^+$ and $[K(15\text{-crown-5})_2]^+$, were obtained. The synthesis of these compounds followed a general procedure (Scheme 1) that is similar to that previously described for the other $[Ni(\alpha\text{-tpdt})_2]^-$ complexes, where 5,6-thieno[2,3-*d*]-1,3-dithiol-2-one (**1**) was reacted with nickel chloride in a basic alcoholic solution and the complexes were isolated as salts by precipitation upon the addition of the cation salt. These reactions were carried out under strictly anaerobic conditions inside a glove box. The reaction with $[K(18\text{-crown-6})]^+$ afforded $[K(18\text{-crown-6})][[Ni(\alpha\text{-tpdt})_2]$ (**3**) as dark green plates in a reasonable yield (74%) after recrystallisation in dichloromethane/*n*-hexane. In contrast to the synthesis with the larger crown-ether, the synthesis with the smaller cation $[K(15\text{-crown-5})_2]^+$ gave an inhomogeneous sample that, after a simple recrystallisation in dichloromethane, remained a mixture of three compounds, namely, $[K(15\text{-crown-5})_2][Ni(\alpha\text{-tpdt})_2]$ (**4**), $[K(15\text{-crown-5})_2]_2[Ni_4(\alpha\text{-tpdt})_6]$ (**5**) and bisthieno[2,3-*c*:2′,3′-*g*][1,2,5,6]tetrathiocine (**6**) (Scheme 1).

These species were clearly distinguishable by their different crystalline morphologies and colour but proved difficult to separate. Compounds **4**, **5** and **6** were obtained as green plate-shaped crystals, dark four-pointed star-shaped crystals and yellow plate crystals, respectively (Supporting Information, Figure S1). These compounds could not be separated by further recrystallisation except for **4**, which was enriched and obtained almost pure by multiple recrystalisations in dichloromethane. The formation of the dianionic Ni_4 cluster **5** from **2** (and/or **4**) implied that two ligands were lost and resulted in the formation of **6**, which was indeed isolated, which suggests that a possible oxidation mechanism occurred through the formation of this partially oxidised cluster. The α-tpdt ligand is known to be able to stabilise high oxidation states of the complexes with different transition metals and often the dianionic complexes are easily oxidised to monoanionic or even to the neutral state by iodine or simply by exposure to air.[11] Indeed, in this study the neutral complex **7** was obtained as a dark microcrystalline powder by the oxidation of **3** or **4** with iodine. However, in contrast to the Au analogue,[11a] this compound was found to be a bad electrical conductor with a conductivity of approximately 10^{-9} S cm^{-1}, which was measured for a powder-compacted sample at room temperature.

The formation of cluster **5** from **2** corresponds to the partial oxidation of the Ni atoms. It was not possible to obtain a pure sample of **5** for the electrochemical studies but a redox process that was associated with the cluster was observed in the cyclic voltammetry studies in a dichloromethane solution of the crystallisation products that contained **5**. The voltammograms revealed a quasireversible redox process that was centred at –0.095 V (vs. Ag/AgCl) between the waves ascribed to the couples $[Ni(\alpha\text{-tpdt})_2]^{2-}$/$[Ni(\alpha\text{-tpdt})_2]^-$ and $[Ni(\alpha\text{-tpdt})_2]^-$/$[Ni(\alpha\text{-tpdt})_2]^0$ at –0.480 and +0.286 V, respectively. The waves of the latter couple have been previously described for the $[Ni(\alpha\text{-tpdt})_2]^-$ acetonitrile solutions,[10a] but this extra redox process was not observed in acetonitrile or with other cations (Supporting Information, Figure S2). Therefore, both the solvent used and the counter cation size seem to contribute to the stabilisation of the cluster.

Compounds **3**–**6** were characterised by single-crystal X-ray diffraction. In the crystal structure of **3** the unit cell contains one independent $[Ni(\alpha\text{-tpdt})_2]^-$ anion (Figure 1) and one independent $[K(18\text{-crown-6})]^+$ cation, with both the K and the Ni atoms located at inversion centres. The potassium ion is in a nearly planar crown-ether environment. Within experimental error, the $[Ni(\alpha\text{-tpdt})_2]^-$ anion is planar and presents disorder in the sulfur atom of the thiophenic ring. This disorder can be either *cis-trans* or positional disorder of the *trans* configuration, which seems to be the more stable one in previous salts.[10,11] The Ni–S bond lengths, with an average value of 2.156(4) Å, are identical to those previously found in the $[Ni(\alpha\text{-tpdt})_2]^-$ anions[10] and are typical of monoanionic Ni dithiolates.[12,13] The crystal structure of **3** consists of alternating cationic and anionic layers (Figure 2, a) and has short interlayer contacts that define the alternating cation-anion chains along *c* (Figure 2, b). Along these chains, the anions

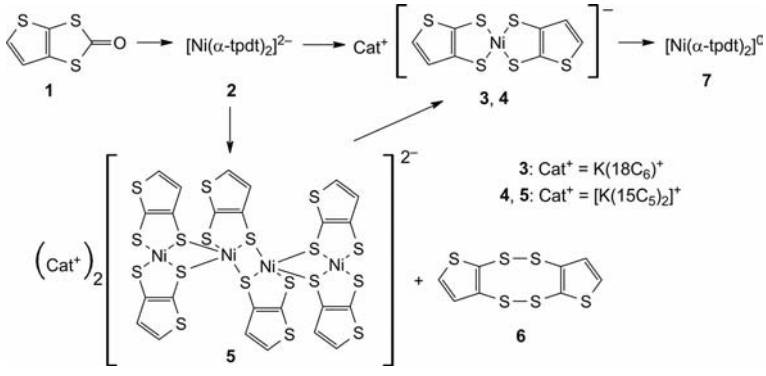

Scheme 1. The preparation of the salts **3**, **4**, **5**, **6** and **7**.

and the cations are linked by very short K···S3 and K···C10 contacts, which are in the range of 3.3 to 3.6 Å, that denote very strong interactions. In the anionic layers S1···S3 and S3A···S3 short contacts are observed, which builds a 2D network of anionic interactions in the *b,c* plane (Figure 2, c). However, this network of contacts is also disordered due to the thiophenic ligand conformational disorder.

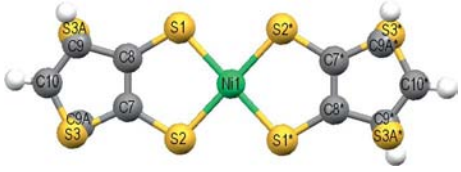

Figure 1. The molecular diagram of the $[Ni(\alpha\text{-tpdt})_2]^-$ anion in **3**.

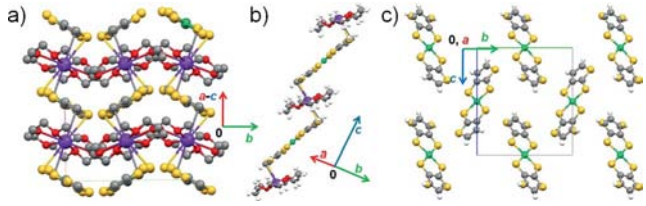

Figure 2. The crystal structure of **3** (a) viewed along *c* (the hydrogen atoms were omitted for clarity); details showing (b) a cation-anion chain and (c) an anionic layer.

Compound **4** was the compound that was initially expected from the reaction of $[Ni(\alpha\text{-tpdt})_2]^-$ with the $[K(15\text{-crown-}5)_2]^+$ cation. Although the crystal quality did not allow a high-quality refinement of the crystal structure, we were able to assert from the X-ray diffraction data that the anionic complex presents the usual square planar coordination geometry for the Ni atom in a *trans* configuration and that the parameters are identical to those found in other $[Ni(\alpha\text{-tpdt})_2]^-$ salts (Supporting Information, Figure S10, Table S3).[10] The K^+ cation is sandwiched between two crown-ether units, which appear to be highly disordered. The crystal packing is composed of columns of alternating pairs of cations and anions along *c*. The molecules in the neighbouring columns are out-of-registry (see Supporting Information, Figure S11a). The pairs of anions are organised in double chains that run parallel to the *b,c* plane and are connected by S···H–C hydrogen bonds and short S···S and S···C interactions (Supporting Information, Figure S11b).

Compound **5**, together with **4**, are coproducts from the reaction that used the $[K(15\text{-crown-}5)_2]^+$ cation. In **5** the nickel dianionic complex has an unexpected geometry, namely, a centrosymmetrical in-line Ni_4 cluster (Figure 3). The peripheral nickel atoms, in addition to a square planar MS_4 coordination, are close to another Ni atom [Ni–Ni, 2.756(2) Å], while the inner Ni atoms {besides the two short Ni–Ni contacts [2.756(2) and 3.142(3) Å]} are coordinated by five sulfur atoms, two of which are from an inner dithiothiophene ligand L3 (S7–9, C9–12) and the other three sulfur atoms that belong to the different neighbouring ligands L1 (S1–3, C1–C4) and L2 (S4–6, C5–8), in a M–S 4+1 coordination geometry (Figure 3). In spite of some evidence for disorder in the thiophenic S9 atom position of the L3 ligand, this disorder could not be modelled in the structural refinement.

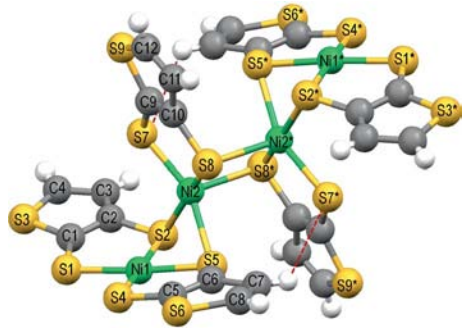

Figure 3. The $[Ni_4(\alpha\text{-tpdt})_6]_2^-$ cluster in **5**. Selected bonds lengths: Ni1–S1 [2.191(5) Å], Ni1–S2 [2.177(6) Å], Ni1–S4 [2.191(6) Å]; Ni1–S5 [2.190(5) Å]; Ni2–S2 [2.327(4) Å]; Ni2–S5 [2.328(4) Å], Ni2–S7 [2.224(4) Å]; Ni2–S8 [2.209(4) Å]; Ni2–S8* [2.415(6) Å]; Ni1–Ni2 [2.754(3) Å]; Ni2–Ni2* [3.140(3) Å]; C7–H7···S7* [2.994(5) Å], where * represents $2 - x$, $1 - y$, $-z$.

The average Ni–S bonds are significantly different for the external Ni1 and internal Ni2 bonds [2.189(5) and 2.272(4) Å, respectively], which suggests that the two nickel atoms possibly have different oxidation states. The bond lengths within the dithiothiophene ligand are comparable to those previously reported[10,11] and also to those found in monoanionic salts **3** and **4**. Around Ni1, the ligands L1 and L2 adopt a boat conformation and their mean planes make a dihedral angle of 18°. The mean plane of the L3 ligand, which is directly bonded to Ni2, is almost perpendicular to the mean planes of L1 and L2, with dihedral angles of 83 and 78°, respectively (Figure 3). It is worth noting the relatively short intermolecular hydrogen bond for C7–H7···S7* of 2.994(5) Å. In the cation, as in **4**, the potassium ion is trapped between two crown-ether units, both of which appear to be slightly disordered. The crystal structure of **5** is composed of parallel chains of clusters that are surrounded by cations (Figure 4, b). There are no interactions between the chains and the cations but the anions are connected by a few hydrogen bonds. The clusters in these chains interact through the S6···S8 short contact [3.54(2) Å] that occurs between the L3 coordinating and the L2 thiophenic sulfur atoms (Figure 4, a). The thiophenic rings of L2 overlap along the chains, which allows significant π–π interactions.

Compound **6** is a coproduct that was obtained with **4** and **5** due to the presence of the free ligand that was generated by the formation of cluster **5**. In fact, the formation of the eight-membered bis(disulfide) rings from the reaction of the *ortho*-dithiolates is not unprecedented.[14] The crystal structure of **6** revealed a 50% *cis*-*trans* disorder of the thiophene rings in a chair-type conformation, as was previously observed for bis(*o*-phenylene) bis(sulfide) (see Supporting Information, Figure S10).[15] The bis(α-thiophene) bis(disulfide) units are arranged in out-of-registry chains that run

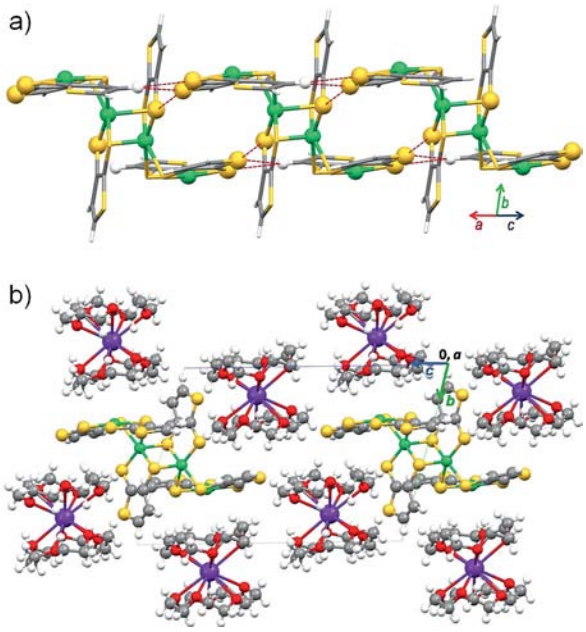

Figure 4. (a) Chains of the $[Ni_4(\alpha\text{-tpdt})_6]^{2-}$ dianionic clusters in **5** that show the interanionic S8···S6* short contacts [3.54(2) Å] and the charge-assisted S···H–C hydrogen bonds [C3–H3···S4** (2.94 Å) and C3–H3···S6* *(2.79 Å)]. The Ni, S and H atoms that are involved in the short contacts are highlighted and are represented as spheres, * represents –1 + *x*, *y*, *z*; and ** represents 1 – *x*, 1 – *y*, –*z*. (b) The crystal structure of **5** viewed along *a*.

parallel to *b*. These species are connected by short S···S interactions along these chains, while the neighbouring chains interact through the C–H···S hydrogen bonds (Figure 5).

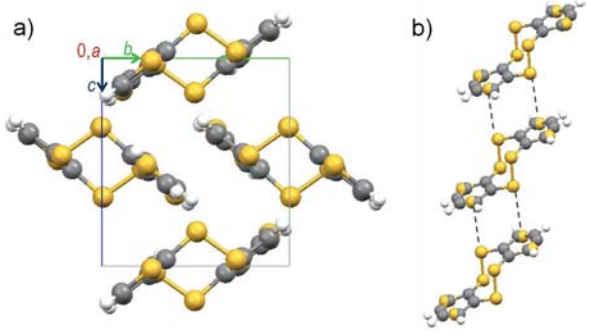

Figure 5. (a) The crystal structure of **6** viewed along *a*; (b) the details of one of the $C_8H_4S_6$ molecular chains in the crystal structure of **6**. The dashed lines represent the short S···S contacts between the molecules ($d_{S\cdots S}$ = 3.017 Å; symmetry operation: 1 – *x*, –*y*, 1 – *z*).

Paramagnetic compounds **3** and **4** were characterised by magnetisation and alternating current (AC) susceptibility measurements. The χ_pT product of **3** was measured under an applied field of 2 T (Figure 6) and is almost constant at 0.364 emu K mol^{-1} (which corresponds to an effective moment, μ_{eff} = 1.71 μ_B) in the range of 40 to 300 K, which is close to the ideal value of 0.40 emu K mol^{-1} (μ_{eff} = 1.79 μ_B) for a S = 1/2 system with $<g>$ = 2.07.[10a] A maximum in the χ_pT product was observed at 25 K. There was a steep decrease in the χ_pT product below this temperature.

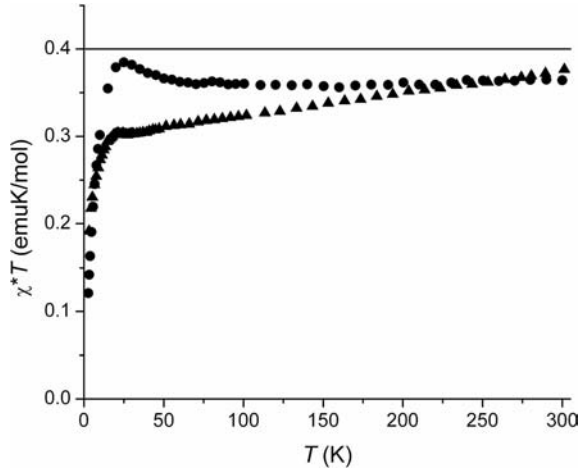

Figure 6. The χT temperature-dependence of [K(18-crown-6)][Ni(α-tpdt)$_2$] (**3**) (circles) and [K(15-crown-5)$_2$][Ni(α-tpdt)$_2$] (**4**) (triangles). The solid line represents the ideal value of 0.4 emu K mol^{-1} for a S = 1/2 system with $<g>$ = 2.07.

The magnetic susceptibility of **3** above 30 K follows a Curie–Weiss behaviour with an effective magnetic moment (μ_{eff}) of 1.7 μ_B and a positive Curie temperature (θ = 1.0 K), which denotes dominant weak ferromagnetic (FM) interactions (Supporting Information, Figure S3). At lower temperatures, a field-dependent maximum was observed for the temperature-dependence of the magnetisation (Figure 7). This maximum shifted to lower temperatures as the field increased until, for applied fields above 0.1 T, it almost disappeared (see inset).

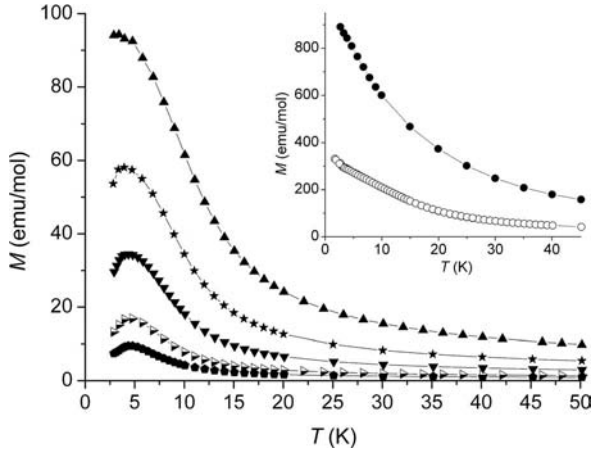

Figure 7. The temperature-dependent magnetisation of [K(18-crown-6)][Ni(α-tpdt)$_2$] (**3**) under the different magnetic fields of 0.005 (pentagons), 0.01(white and black triangles), 0.025(inverted triangles), 0.05 (stars), 0.1 (triangles), 0.5 (open circles) and 2 T (circles).

The isothermal magnetisation curves for **3** at different temperatures (Supporting Information, Figure S4) showed that between 20 and 5 K the experimental values at the low fields are larger than those calculated from the Brillouin function for a system of independent S = 1/2 spins. However, at the higher fields the results are smaller than those

calculated from the Brillouin function. At temperatures above 50 K, the magnetisation exceeds the Brillouin function at very low magnetic fields, while at 1.6 K the magnetisation is always smaller than the calculated values. These results suggest that there is a competition between the ferromagnetic and antiferromagnetic interactions.

The magnetisation cycle of **3** at 1.6 K (Figure 8) presents a hysteresis of the order of 500 G and at 5 T attains a magnetisation of 0.39 μ_B, which is far from saturation. These results could be due to a glassy-type behaviour for the magnetisation below the freezing temperature, T_f, which is possibly associated with a cluster-glass behaviour that has already been observed in the other salts that are based on the $[Ni(\alpha\text{-tpdt})_2]^-$ anion and that have a similar ligand disorder.[10]

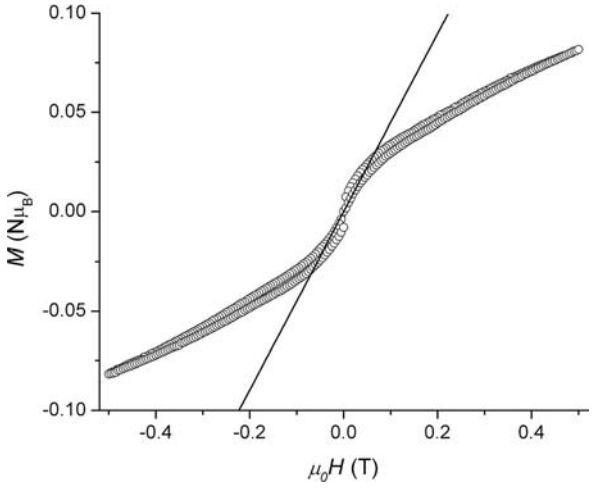

Figure 8. The magnetisation curve of [K(18-crown-6)][Ni(α-tpdt)$_2$] (**3**) at 1.6 K. The solid line represents the calculated Brillouin function for the S = 1/2 system with <g> = 2.07.

The presence of such a freezing process was confirmed by AC susceptibility measurements. Indeed, χ_{AC} data that was taken under a zero-applied direct current (DC) field at different frequencies in the range of 33 to 9995 Hz (Figure 9) showed a temperature dependence and distinct peaks in both the real χ' and the imaginary χ'' components of χ_{AC}. At the lowest frequency, 95 Hz, the maximum in χ' occurs at 6.5 K, while in χ'' this maximum is shifted to a lower temperature, namely, 5.8 K. These peaks in both the real and the imaginary components are consistent with the existence of a weak ferromagnetism below 6.5 K, which has already been suggested by the DC magnetisation measurements.

Both the real and the imaginary components of χ_{AC} exhibit a strong shift with the change in frequency, ω. The peak temperatures are shifted to higher temperatures while their height decreases as the frequency increases. This type of shift is characteristic of glassy systems and is a result of the slow relaxation processes and the freezing into a non-equilibrium state below the frequency-dependent temperature T_f. This freezing temperature, T_f, which is given by the maximum in the AC susceptibility, is frequency-dependent

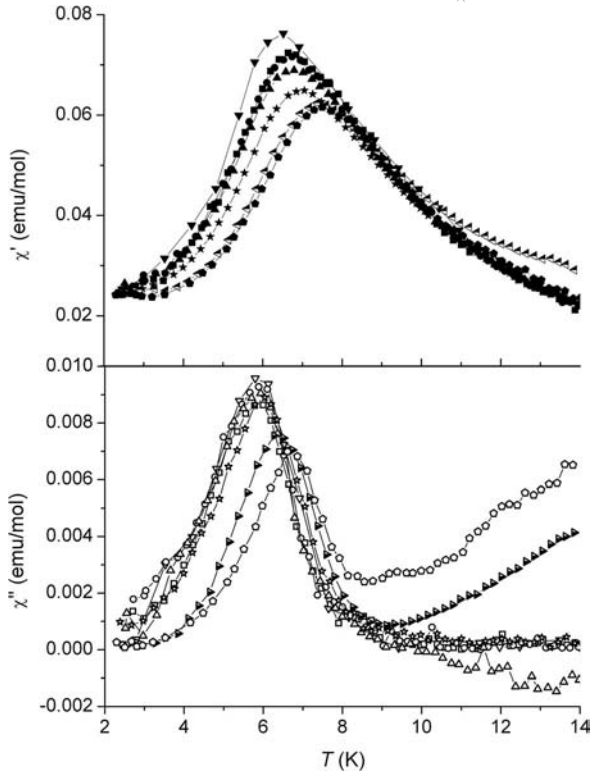

Figure 9. The temperature-dependent χ'(top) and χ'' (bottom) for [K(18-crown-6)][Ni(α-tpdt)$_2$] (**3**) at the different frequencies of 95 (inverted triangles), 333 (squares), 495 (circles), 995 (triangles), 3330 (stars), 4995 (white and black triangles) and 9995 Hz (pentagons), where χ' has the filled symbols and χ'' has the open symbols.

and its change, ΔT_f, follows the empirical law $\Psi = (\Delta T_f/T_f)/\Delta(\log\omega)$[16] with $\Psi \approx 0.09$, which is a value that is consistent with the cluster-glass behaviour.

A number of external DC fields were applied in order to determine the evolution of the transition with the magnetic field for the AC measurements. The temperature-dependence of χ_{AC} that was taken at 995 Hz with a H_{AC} of 1 Oe and different applied DC fields is shown in Figure S5 of the Supporting Information. These results suggested that the application of an external magnetic DC field decreases the intensity of the peak and shifts the maximum to lower temperatures. For fields that are higher than 500 G, the peaks are almost suppressed. This particular behaviour can also be attributed to the existence of cluster domains that have short-range order.

The effective magnetic moment of **4** is 1.74 μ_B at room temperature, which is close to 1.79 μ_B that was calculated for a system of independent S = 1/2 spins with <g> = 2.07. However, upon cooling the value gradually decreases until 25 K (Figure 6), which indicates that the antiferromagnetic interactions are predominant at high temperatures. Below 20 K, a faster decrease is observed. The magnetic susceptibility above 50 K follows a modified Curie–Weiss law (Supporting Information, Figure S6) with a TIP (temperature-independent paramagnetism) of 2.5×10^{-5} emu mol^{-1} and a negative Curie temperature (θ = –0.42 K).

The isothermal magnetisation of **4** at 1.7 K (Figure 10) showed no signs of hysteresis and 0.25 μ_B was attained at 3 T, which is far from saturation and well below the calculated Brillouin function for the independent $S = 1/2$ spins, which indicates that significant antiferromagnetic interactions exist. For the other temperatures, it was possible to verify a linear dependence of the magnetisation with the magnetic field, which is typical of a system with antiferromagnetic (AFM) interactions, and that had values that were always smaller than the calculated Brillouin function.

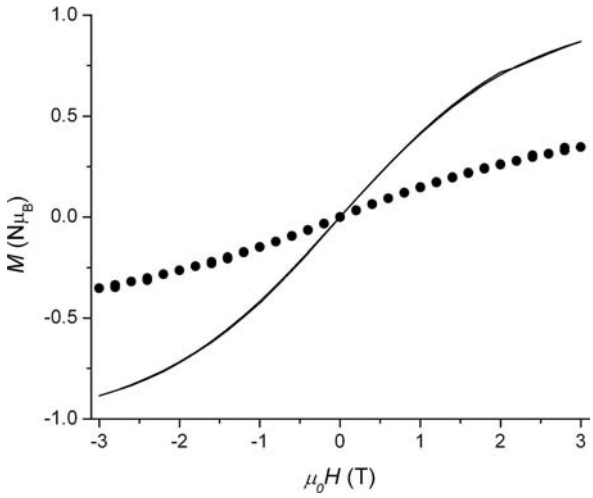

Figure 10. The magnetisation of $[K(15\text{-crown-}5)_2][Ni(\alpha\text{-tpdt})_2]$ (**4**) at 1.7 K. The solid line represents the calculated Brillouin function for a system of $S = 1/2$ spin with $<g> = 2.07$.

The AC susceptibility measurements at low temperatures and at different frequencies were also performed for compound **4**. A less pronounced frequency dependence was observed for compound **4** than that found for compound **3** as is shown in Figure S7 of the Supporting Information. In both the real χ' and the imaginary χ'' components small maxima were observed around 7 and 6 K, respectively, which is consistent with the presence of weak ferromagnetism. The poor signal/noise ratio did not allow a precise determination of the Ψ parameter. Nevertheless, this frequency-dependence of the AC susceptibility still supports the occurrence of metastability in the magnetic anion layers with a tendency to induce cluster formation.

The type of magnetic interactions between the $[Ni(\alpha\text{-tpdt})_2]^-$ anions can be predicted, as previously done in other salts of this anion, from the calculated spin density distribution in this complex[10c,10d] (Supporting Information, Figure S9) by using the McConnell I mechanism.[17] A competition between the FM and AFM interactions (with variable intensities estimated) in both **3** and **4** were predicted by this analysis (Supporting Information, Figure S13 and Tables S5 and S6).

The magnetic behaviour in **3** is therefore dominated by this competition and also by the molecular disorder observed in the thiophenic sulfur atom of the anionic species. It is worth noting that this disorder does not change the type of interaction, which remains FM, however, depending on the molecular configuration, these FM interactions can differ in their strength, which possibly enables different FM domains. Thus, the ligand disorder results in a macroscopic FM cluster-glass behaviour. Competition between the FM and AFM interactions is also expected for compound **4**. At high temperatures the AFM interactions dominate, as can be seen by the decrease in χT upon cooling. In χ_{AC} there is an anomaly that suggests an "ordering" process at approximately 6 K, which is similar to that observed for **3**, however, the frequency shift of the peaks is not as evident in this case. Most probably the lower dimensionality of this system, in which there are isolated double chains instead of layers, softens the ordering process.

The bulky polycrystalline samples of compound **5** could not be magnetically characterised due to the difficulty that was experienced in obtaining large enough quantities of the pure samples. However, the single crystals were found to be EPR silent, which suggests a diamagnetic ground state as a result of the antiferromagnetically-coupled Ni^{III} centres.

The Ni atoms in the centrosymmetrical cluster may present two distinct formal oxidation states, namely, two Ni^{II} and two Ni^{III}. Alternatively, in view of the short Ni–Ni distances and strong ligand–metal interactions, the Ni atoms may have a mixed valence/partial oxidation state with electron delocalisation. In order to elucidate the electronic structure of **5**, we started calculations based on Density Functional Theory with different guess functions to cover the possible assignments (see the Computational Details section). The results indicated that the most stable situation corresponds to a singlet determinant with two central Ni^{III} ions that are antiferromagnetically coupled and two external Ni^{II} centres (Figure 11). The central paramagnetic Ni^{III} ions had a calculated J value of $-1867\ cm^{-1}$ (using the $\hat{H} = -J\hat{S}_1\hat{S}_2$ Hamiltonian), which is a very strong antiferromagnetic coupling that is in agreement with the silent EPR spectrum. The spin density is clearly localised in the Ni2 atoms (0.94 e^- each, Supporting Information, Figure S13) in the d_{z^2} orbital, while the value for the Ni^{II} centres is only 0.05 e^-. Despite the long distances between the Ni^{III} cations and the sulfur bridging ligands between the two Ni^{III} centres, the spin delocalisation mechanism is predominant.[18] The mixing of the sulfur atom orbitals with the lobe of the Ni^{III} d_{z^2} orbital that is perpendicular to the plane of the four short Ni–S bond lengths is large enough to overcome the interaction with the torus lobe of the d_{z^2} orbital of the other Ni^{III} cation. For these sulfur atoms, the spin density will have the same sign as that of the Ni^{III} centre. Hence, in the central Ni_2S_2 framework there are two atoms that have spin up and the other two atoms have spin down. Finally, the external Ni^{II} cation and its four coordinated sulfur atoms have a spin density sign that is opposite to that of the closest Ni^{III} centre, which shows the predominance of the polarisation mechanism.[19]

The coordination spheres of the Ni1 and Ni2 atoms are slightly different since, although both are square planar, there is a fifth bridging sulfur atom that has a long distance for the Ni2 atoms. Hence, the electronic structure adopted for this complex corresponds to a class 1 mixed-valence

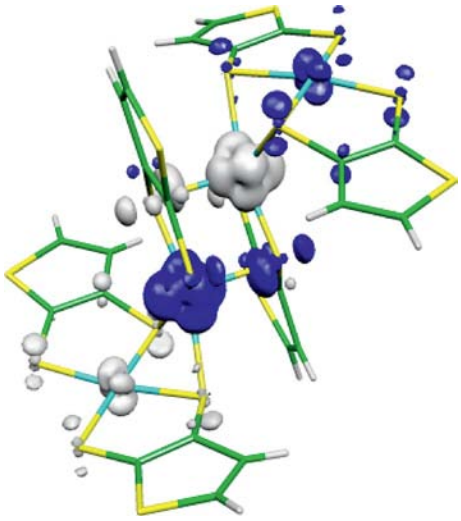

Figure 11. A representation of the calculated spin density for the dianionic cluster in **5** by using isosurfaces of 0.005 e^-.

complex according to the Robin–Day classification.[19] It is worth noting the very strong coupling by taking into account the presence of two relatively long Ni–S distances in the bridging ligands [2.415(6) Å] and the topology of the "magnetic orbitals".

In order to analyse the possible metal–metal interactions, an atoms-in-molecules study[20] was done. No bond critical points were found in the centre of the three distorted rhombus Ni_2S_2 structures. In all of the cases they correspond to ring critical points that indicate the lack of direct metal–metal interactions. The molecular orbital analysis agreed with these conclusions. At first glance, by taking into account the coordination of five of the Ni^{III} ions, we can consider that the full d_{z^2} orbital of the terminal Ni^{II} centres would act as a ligand completing the coordination of the Ni^{III} ions until six. In this case, its interaction with the singly-occupied Ni^{III} d_{z^2} orbital would result in a distorted octahedron coordination polyhedra for the central Ni^{III} ions. However, the antibonding combinations of the d_{z^2} orbitals of the Ni^{II} and Ni^{III} cations (Supporting Information, Figure S8) are occupied, which therefore confirms the absence of strong metal–metal interactions. The existence of the intramolecular C–H···S hydrogen bonds (red dashed lines in Figure 4) was confirmed by the presence of the bond critical points. They can contribute to the non-planarity of the external Ni_2S_2 framework.

Conclusions

In summary, a series of new compounds that are based on nickel complexes with the thiophene-2,3-dithiolate ligand and the crown-ether cations, $[K(18\text{-crown-6})]^+$ and $[K(15\text{-crown-5})_2]^+$, were obtained. The magnetic properties of the salts **3** and **4**, based on the paramagnetic $[Ni(\alpha\text{-tpdt})_2]^-$ anions in the usual square planar coordination geometry, are dominated by a competition between the AFM and FM interactions. However, a magnetic cluster-glass behaviour was observed at temperatures below 6 K due to ligand *cis-trans* disorder. This glass behaviour is more pronounced in the salt with the $[K(18\text{-crown-6})]^+$ cation, which presents the typical structure that consists of anionic layers, than in the $[K(15\text{-crown-5})_2]^+$ salt, which has a new structure type that consists of anionic double chains.

For the $[K(15\text{-crown-5})_2]^+$ cation, an unprecedented in-line Ni_4–S_{12} cluster that had relatively short Ni–Ni distances was also obtained and was characterised by single-crystal X-ray diffraction. This cluster results from an unstable equilibrium between the regular square planar monoanionic and dianionic bidithiolenes, which is favoured by both the solvent and the cation. The structural and computational data indicated that in this cluster there is no direct Ni–Ni interaction and that the outer nickel atoms are Ni^{II} while the central ones are Ni^{III} in a class 1 mixed-valence complex according to the Robin–Day classification.

Experimental Section

General Experimental Conditions: All of the manipulations were carried out under strict anaerobic conditions under a dry nitrogen or argon atmosphere, unless otherwise stated. All of the solvents were purified and dried by following standard procedures. The other chemicals were obtained commercially and were used without any further purification.

$[K(18\text{-crown-6})][Ni(\alpha\text{-tpdt})_2]$ (3): A similar methodology to the one that was previously reported[10a] for the synthesis of the $n$$Bu_4N$-$[Ni(\alpha\text{-tpdt})_2]$ salt was followed. A solution of 18-crown-6 (2 equiv.) in methanol was added to a solution of $[Ni(\alpha\text{-tpdt})_2]^-$ in methanol immediately after oxidation by air exposure. Compound **3** was obtained in 74% yield by the recrystallisation of the salt from a dichloromethane solution in an atmosphere that was saturated with n-hexane. $C_{20}H_{28}KNiO_6S_6$ (654.61): calcd. C 36.70, H 4.31, S 29.39; found C 35.47, H 4.26, S 29.44.

$[K(15\text{-crown-5})_2][Ni(\alpha\text{-tpdt})_2]$ (4): A similar methodology to the one that was previously reported[10a] for the synthesis of the $n$$Bu_4N$-$[Ni(\alpha\text{-tpdt})_2]$ salt was followed. A solution of 15-crown-5 (2 equiv.) in methanol was added to the solution of $[Ni(\alpha\text{-tpdt})_2]^-$ in methanol immediately after oxidation by air exposure. The inhomogeneous sample was purified by recrystallisation from a dichloromethane solution in an atmosphere that was saturated with n-hexane to yield a mixture of crystals of **4**, **5** and **6**, which could be clearly distinguished from one another. Further recrystallisation of the salts in dichloromethane afforded a sample that consisted almost entirely of **4**. $C_{28}H_{44}KNiO_{10}S_6$ (830.82): calcd. C 40.48, H 5.34, S 23.15; found C 40.26, H 6.12, S 22.69.

$[Ni(\alpha\text{-tpdt})_2]^0$ (7): A solution of iodine (18 mg, 7.12×10^{-2} mmol) in acetone (2 mL) was added dropwise to a solution of $n$$Bu_4N$-$[Ni(\alpha\text{-tpdt})_2]$ (50 mg, 1.4×10^{-1} mmol) or **3** (91 mg,1.4×10^{-1} mmol) in acetone (2 mL). The resulting dark precipitate was isolated by centrifugation, washed with acetone and dried in vacuo to yield **7** (19 mg) in 31% yield. $C_8H_4NiS_6$ (351.19): calcd. C 27.36, H 1.15, S 54.77; found C 27.40, H 1.10, S 53.98.

X-ray Diffraction: The experiments were performed with a Bruker AXS APEX CCD detector diffractometer by using graphite-monochromated Mo-K_α radiation (λ = 0.71073 Å) in the ϕ and ω scan modes. A semi-empirical absorption correction was carried out with SADABS.[21] The data collection, cell refinement and data re-

duction were done with the SMART and SAINT programs.[22] The structures were solved by direct methods with SIR97[23] and were refined by full-matrix least-squares methods with the program SHELXL97[24] with the winGX software package.[25] The non-hydrogen atoms were refined with anisotropic thermal parameters whereas the H-atoms were placed in idealised positions and were allowed to be refined riding on the parent C atom. The molecular graphics were prepared with ORTEP 3.[26]

Crystallographic data for 3: $C_{20}H_{28}O_6S_6KNi$, M_r = 654.60 g mol^{-1}, monoclinic, space group $P2_1/n$, a = 9.449(5) Å, b = 11.474(5) Å, c = 12.839(5) Å, β = 94.589(5)°, V = 1387.5(11) Å^3, Z = 4, D_c = 1.567 g cm^{-3}, μ(Mo-K_α) = 1.334 mm^{-1}, 2723 reflections measured, 733 unique, final $R(F^2)$ = 0.08 using 733 reflections with $I > 2.0\sigma(I)$, R(all data) = 0.11, T = 293(2) K.

Crystallographic Data for 4: $C_{28}H_{44}O_{10}S_6KNi$, M_r = 810.94 g mol^{-1}, monoclinic, space group $P2_1/c$, a = 23.979(3) Å, b = 32.230(5) Å, c = 9.5921(14) Å, β = 94.751(5)°, V = 7387.9(2) Å^3, Z = 8.

Crystallographic Data for 5: $C_{64}H_{92}K_2Ni_4O_20S_{18}$, M_r = 2071.5 g mol^{-1}, triclinic, space group $P\bar{1}$, a = 9.964(2) Å, b = 12.754(2) Å, c = 18.597(3) Å, α = 73.971(3)°, β = 83.578(4)°, γ = 86.982(4)°, V = 2256.7(6) Å^3, Z = 2, D_c = 1.524 g cm^{-3}, μ(Mo-K_α) = 1.391 mm^{-1}, 11251 reflections measured, 7498 unique, final $R(F^2)$ = 0.13 using 2005 reflections with $I > 2.0\sigma(I)$, R(all data) = 0.26, T = 150(2) K.

Crystallographic Data for 6: $C_8H_4S_6$, M_r = 292.47 g mol^{-1}, monoclinic, space group $P2_1/n$, a = 7.9380(6) Å, b = 7.9112(7) Å, c = 8.7670(7) Å, β = 96.076(3)°, V = 547.47(8) Å^3, Z = 2, D_c = 1.774 g cm^{-3}, μ(Mo-K_α) = 1.201 mm^{-1}, 2265 reflections measured, 912 unique, final $R(F^2)$ = 0.03 using 809 reflections with $I > 2.0\sigma(I)$, R(all data) = 0.03, T = 150(2) K.

CCDC-830009 (for **3**), -761154 (for **5**) and -761155 (for **6**) contain the supplementary crystallographic data for this paper. These data can be obtained free of charge from The Cambridge Crystallographic Data Centre via www.ccdc.cam.ac.uk/data_request/cif.

Magnetic Measurements: The experiments were performed with a S700X SQUID magnetometer with a 70 kG magnet (Cryogenic Ltd.) with the polycrystalline samples. The temperature dependence of the magnetic susceptibility in the temperature range of 5 to 320 K was measured under a magnetic field of 10 kG. A Maglab 2000 system (Oxford Instruments) was used for the AC susceptibility measurements down to 1.5 K in the frequency range of 99 to 9990 Hz and with a 1 G AC field. The paramagnetic susceptibility was obtained from the experimental magnetisation data after a diamagnetism correction was estimated from the tabulated Pascal constants.

Computational Details: The electronic structure calculations were based on Density Functional Theory methods and were performed by using the hybrid B3LYP functional[27] and the all electron triple-ζ basis set[28] with the NWChem. code.[29] In order to generate all of the possible combinations for the oxidation states of the nickel atoms, the Jaguar code[30] was employed to obtain the starting guess functions by using the approach proposed by Vacek et al.[31] The atoms-in-molecules analysis was performed by using the AIMall code[32] with the wavefunction generated with the Gaussian03 revision D02[33] code for the more stable case.

Supporting Information (see footnote on the first page of this article): The details of the synthesis (Figure S1), cyclic voltammetry (Figure S2), crystal structure analysis (Figures S10 to S12) and the magnetic characterisation of compounds **3**, **4** and **5** (Figures S3 to S9 and S13) are presented. Tables with the atomic distances (Tables S1 to S4) and with the analysis of the short intermolecular (Tables S5 and S6) contacts in **3** and **4** are also presented.

Acknowledgments

This work was partially supported by Portuguese Fundação do Ministério de Ciência e Tecnologia (FCT) under contracts POCI/QUI/57528/2004 and PDCT/QUI/ 64967/2006 and we also benefitted from the European Cooperation in the Field of Science and Technology (COST), D35. E. R. and C. R. thank the Spanish Ministerio de Ciencia e Innovación (MICINN) (grant numbers CTQ2008-06670-C02-01 CTQ2010-19501) and the Direcció General de Recerca (DGR) (grant numbers 2009SGR-1459 and 2009SGR-108). E. R. also thankfully acknowledges the computer resources, technical expertise and assistance provided by the Barcelona Supercomputing Centre (Centro Nacional de Supercomputación).

[1] a) J. A. McCleverty, *Prog. Inorg. Chem.* **1968**, *10*, 49–221; b) U. T. Mueller-Westerhoff, B. Vance, in: *Comprehensive Coordination Chemistry* (Eds.: G. Wilkinson, R. D. Gillard, J. A. McCleverty), Pergamon, Oxford **1987**; c) D. Coucouvanis, *Prog. Inorg. Chem.* **1970**, *11*, 233–371; d) L. Alcácer, H. Novais, in: *Extended Linear Chain Compounds* (Ed.: J. S. Miller), Plenum Press, New York, **1983**, vol. 3, pp. 319–351; e) P. I. Clemenson, *Coord. Chem. Rev.* **1990**, *106*, 171–203; f) A. E. Pullen, R.-M. Olk, *Coord. Chem. Rev.* **1999**, *188*, 211–262; g) N. Robertson, L. Cronin, *Coord. Chem. Rev.* **2002**, *227*, 93–127; h) R. Kato, *Chem. Rev.* **2004**, *104*, 5319–5346.

[2] a) C. L. Beswick, J. M. Schulman, E. I. Stiefel, *Prog. Inorg. Chem.* **2004**, *52*, 55; b) S. Alvarez, R. Vicente, R. Hoffman, *J. Am. Chem. Soc.* **1985**, *107*, 6253–6277.

[3] a) D. Simão, H. Alves, D. Belo, S. Rabaça, E. B. Lopes, I. C. Santos, V. Gama, M. T. Duarte, R. T. Henriques, H. Novais, M. Almeida, *Eur. J. Inorg. Chem.* **2001**, 3119–3126; b) X. Ribas, J. C. Dias, J. Morgado, K. Wurst, M. Almeida, T. Parella, J. Veciana, C. Rovira, *Angew. Chem.* **2004**, *116*, 4141; *Angew. Chem. Int. Ed.* **2004**, *43*, 4049–4052.

[4] V. Gama, R. T. Henriques, M. Almeida, L. Veiros, M. J. Calhorda, A. Meetsma, J. L. de Boer, *Inorg. Chem.* **1993**, *32*, 3705–3711.

[5] V. Gama, R. T. Henriques, G. Bonfait, M. Almeida, A. Meetsma, S. Van Smaalen, J. L. de Boer, *J. Am. Chem. Soc.* **1992**, *114*, 1986–1989.

[6] J. G. Breitzer, T. B. Rauchfuss, *Polyhedron* **2000**, *19*, 1283–1291.

[7] a) B. S. Snyder, C. P. Rao, R. H. Holm, *Aust. J. Chem.* **1986**, *39*, 963; b) J. R. Nicholson, G. Christou, J. C. Huffman, K. Folting, *Polyhedron* **1987**, *6*, 863–870.

[8] T. Sheng, X. Wu, W. Zhang, Q. Wang, X. Ga, P. Lin, *Chem. Commun.* **1998**, 263–264.

[9] a) G.-E. Matsubayashy, A. Yokozawa, *J. Chem. Soc., Chem. Commun.* **1991**, 68–69; b) J. Dai, M. Munakata, Y. Ohno, G. Q. Bian, Y. Suenaga, *Inorg. Chim. Acta* **1999**, *285*, 332–335; c) J. R. Nicholson, I. L. Abrahams, W. Clegg, C. D. Garner, *Inorg. Chem.* **1985**, *24*, 1092–1096; d) D. Belo, M. J. Figueira, J. Mendonça, I. C. Santos, M. Almeida, R. T. Henriques, M. T. Duarte, C. Rovira, J. Veciana, *Eur. J. Inorg. Chem.* **2005**, 3337–3345.

[10] a) D. Belo, H. Alves, S. Rabaça, L. C. Pereira, M. T. Duarte, V. Gama, R. T. Henriques, M. Almeida, E. Ribera, C. Rovira, J. Veciana, *Eur. J. Inorg. Chem.* **2001**, 3127–2133; b) D. Belo, M. J. Figueira, J. P. M. Nunes, I. C. Santos, L. C. Pereira, V. Gama, M. Almeida, C. Rovira, *J. Mater. Chem.* **2006**, *16*, 2746–2756; c) D. Belo, J. Mendonça, I. C. Santos, L. C. Pereira, M. Almeida, J. J. Novoa, C. Rovira, J. Veciana, V. Gama, *Eur. J. Inorg. Chem.* **2008**, 5327–5337; d) D. Belo, L. C. Pereira, M.

Almeida, C. Rovira, J. Veciana, V. Gama, *Dalton Trans.* **2009**, 4176–4180; e) A. I. S. Neves, J. C. Dias, B. J. C. Vieira, M. B. C. Branco, L. C. J. Pereira, I. C. Santos, J. C. Waerenborgh, M. Almeida, D. Belo, V. Gama, *CrystEngComm* **2009**, *11*, 2160–2168.

[11] a) D. Belo, H. Alves, E. B. Lopes, M. T. Duarte, V. Gama, R. T. Henriques, M. Almeida, A. Pérez-Benítez, C. Rovira, J. Veciana, *Chem. Eur. J.* **2001**, *7*, 511–519; b) D. Belo, M. J. Figueira, J. Mendonça, I. C. Santos, M. Almeida, R. T. Henriques, M. T. Duarte, C. Rovira, J. Veciana, *Eur. J. Inorg. Chem.* **2005**, 3337–3345.

[12] W. E. Broderick, J. A. Thompson, M. R. Godfrey, M. Sabat, B. M. Hoffman, *J. Am. Chem. Soc.* **1989**, *111*, 7656–7657.

[13] C. Mahadevan, M. Seshasayer, P. Kuppusamy, P. T. Manoharan, *J. Cryst. Spectrosc. Res.* **1985**, *15*, 305–316.

[14] L. Field, W. D. Stephens, E. L. Lippert, *J. Org. Chem.* **1961**, *26*, 4782–4783.

[15] E. J. Yearley, E. L. Lippert, D. J. Mitchell, A. A. Pinkerton, *Acta Crystallogr., Sect. C* **2007**, *63*, o576–577.

[16] J. A. Mydosh, *Spin Glasses: An Experimental Introduction*, Taylor & Francis, London, **1993**.

[17] H. M. McConnell, *J. Chem. Phys.* **1963**, *39*, 1910.

[18] J. Cano, E. Ruiz, S. Alvarez, M. Verdaguer, *Comments Inorg. Chem.* **1998**, *20*, 27–56.

[19] M. B. Robin, P. Day, *Adv. Inorg. Chem. Radiochem.* **1967**, *10*, 247–422.

[20] R. F. W. Bader, *Atoms in Molecules - A Quantum Theory*, Oxford University Press, Oxford, **1990**.

[21] G. M. Sheldrick, *SADABS*, Bruker AXS Inc., Madison, Wisconsin, USA, **2004**.

[22] Bruker, SMART and SAINT, Bruker AXS Inc., Madison, Wisconsin, USA, **2004**.

[23] A. Altomare, M. C. Burla, M. Camalli, G. Cascarano, G. Giacovazzo, A. Guagliardi, A. G. G. Moliterni, G. Polidori, R. Spagna, *J. Appl. Crystallogr.* **1999**, *32*, 115–119.

[24] G. M. Sheldrick, *SHELXL97*, University of Göttingen, Germany, **1997**.

[25] L. J. Farrugia, *J. Appl. Crystallogr.* **1999**, *32*, 837–838.

[26] L. J. Farrugia, *J. Appl. Crystallogr.* **1997**, *30*, 565.

[27] A. D. Becke, *J. Chem. Phys.* **1993**, *98*, 5648–5652.

[28] A. Schaefer, C. Huber, R. Ahlrichs, *J. Chem. Phys.* **1994**, *100*, 5829–5835.

[29] *NWChem.*, v.4.7: R. A. Kendall, E. Apra, D. E. Bernholdt, E. J. Bylaska, M. Dupuis, G. I. Fann, R. J. Harrison, J. L. Ju, J. A. Nichols, J. Nieplocha, T. P. Straatsma, T. L. Windus, A. T. Wong, *Comput. Phys. Commun.* **2000**, *128*, 260–283.

[30] *Jaguar 7.0*, Schrödinger, Inc., Portland, **2007**.

[31] G. Vacek, J. K. Perry, J.-M. Langlos, *Chem. Phys. Lett.* **1999**, *310*, 189–194.

[32] Todd A. Keith, *AIMAll* (version 11.05.16), TKGristmill Software, Kansas City, USA, **2011**; http://www.aim.tkgristmill.com.

[33] M. J. Frisch, G. W. Trucks, H. B. Schlegel, G. E. Scuseria, M. A. Robb, J. R. Cheeseman, J. A. Montgomery Jr., T.Vreven, K. N. Kudin, J. C. Burant, J. M. Millam, S. S. Iyengar, J. Tomasi, V. Barone, B. Mennucci, M. Cossi, G. Scalmani, N. Rega, G. A. Petersson, H. Nakatsuji, M. Hada, M. Ehara, K. Toyota, R. Fukuda, J. Hasegawa, M. Ishida, T. Nakajima, Y. Honda, O. Kitao, H. Nakai, M. Klene, X. Li, J. E. Knox, H. P. Hratchian, J. B. Cross, V. Bakken, C. Adamo, J. Jaramillo, R. Gomperts, R. E. Stratmann, O. Yazyev, A. J. Austin, R. Cammi, C. Pomelli, J. W. Ochterski, P. Y. Ayala, K. Morokuma, G. A. Voth, P. Salvador, J. J. Dannenberg, V. G. Zakrzewski, S. Dapprich, A. D. Daniels, M. C. Strain, O. Farkas, D. K. Malick, A. D. Rabuck, K. Raghavachari, J. B. Foresman, J. V. Ortiz, Q. Cui, A. G. Baboul, S. Clifford, J. Cioslowski, B. B. Stefanov, G. Liu, A. Liashenko, P. Piskorz, I. Komaromi, R. L. Martin, D. J. Fox, T. Keith, M. A. Al-Laham, C. Y. Peng, A. Nanayakkara, M. Challacombe, P. M. W. Gill, B. Johnson, W. Chen, M. W. Wong, C. Gonzalez, J. A. Pople, *Gaussian 03*, rev. D02, Gaussian Inc., Wallingford CT, **2004**.

Received: July 30, 2011
Published Online: September 15, 2011

